Journal of the Optical Society of Korea, Vol. 8, No. 2, June 2004, pp. 83-89

Variable Optical Fiber Attenuator Using Bending-Sensitive Fiber

Dong-Ho Lee*, Kwang-Hee Kwon, and Jae-Won Song

School of Electronic and Electrical Engineering Kyungpook National University, Daegu, 702-701, South KOREA

Jae-hee Park

Keimyung University Dept. of Electronic Engineering, 1000 Sandang-Dong, Dalseo-Gu, Daegu, 702-701, South KOREA

(Received October 2, 2003)

A variable optical attenuator with a bending-sensitive fiber (*BSF*) that can be used in optical networks is developed. The refractive index profile of the *BSF* is divided into four regions which are inner core, center dip of inner core, outer core and clad. The 3-dimensional finite difference beam propagation method (*3D FD-BPM*) is utilized to find the characteristics of the *BSF*, so the mode profile of the *BSF* and optical power attenuation according to the bending are investigated, and the equivalent model of the *BSF* is made. By using this equivalent model of the *BSF*, the *BSF* is fabricated, and the refractive index profile of the *BSF* is measured, which is similar to refractive index profile of the proposed *BSF*. The fabricated variable optical fiber attenuator (*VOFA*) consists of the *BSF* in a rectangular rubber ring with a fixed bend radius (*BR*) in a steady state. The *VOFA* using the proposed *BSF* was able to attenuate the optical power by more than about *-38 dB* at certain wavelengths (*1540 ~ 1560 nm*) based on adjusting the mechanical pressure applied to the upper surface of the rectangular rubber ring with the bent *BSF*. In addition, the proposed *VOFA* produced an insertion loss of *0.68 dB*, polarization dependent loss (*PDL*) of about *0.5 dB*, and return loss of less than *-60 dB*.

OCIS codes : 230.0230, 060.0060, 060.2340, 060.2400

I. INTRODUCTION

The bending effect, where light traveling in a waveguide scatters away when the *BR* of the waveguide exceeds a critical value, is a well-known mechanism and has already been thoroughly analyzed by many researchers [1-3]. As a result, various optical components have been developed, including variable optical attenuators and polarizers [4-5]. In particular, variable optical attenuators (*VOAs*) are frequently used to adjust the optical power level in many photonic fields, such as reducing crosstalk in switching networks, equalizing the channel power levels in wavelength multiplexed systems, and reducing power fluctuation [5]. Consequently, various types of *VOA* have been developed using microelectromechanical systems (*MEMS*) [6-7], the thermo-optic effect of the polymers [8-10], the coupling effect between two distant fibers [11], and the bending effect in a waveguide [12]. Among these, fiber-type *VOAs* have been found to be particularly appropriate for optical systems, due to easy packaging, low costs, low insertion losses, and reliable attenuation. However, fiber-type *VOAs* also require processes that are difficult to optimize, for example, fusing the fiber, aligning two distant fibers, and adding additional polymer cladding for a thermo-optic effect. Thus, to avoid these problems, a variable optical fiber attenuator (*VOFA*) that utilizes a sharp bend at the heated local region of the *SMF* was developed [12]. Yet, a device with such a sharp bend also requires a process for eliminating the protective coating to heat the local region of the fiber, and moreover, since the bent region can easily be broken due to shock caused by displacement of the *BR*, the fiber requires additional action to protect it from being damaged. However, if the light in the guiding region escapes easily with a large *BR*, these processes are not needed. Generally, two methods of increasing the bending loss are known. One is to make the refractive index of the core lower, yet this method increases the reflection effect because of the difference of refractive index between two coupling fibers. The other is to make the width of the core narrower, but

this method not only increases the difficulty of alignment but also reduces the optical power because of the different radius. Therefore, adding the 2nd core, with refractive index lower than the core and higher than the rest part of the cladding region, to surround the inner core is proposed to make a *BSF* without removing the protective coating. At that time, the optical power of the core can be preserved in the core when there is no bending, but can easily escape from the core to cladding at the local micro-bending because of the existence of the 2nd core which acts as a catalyst for coupling between the core and the cladding. As a result, the bending loss of the *BSF* is much higher than that of the *SMF*. *3D FD-BPM* was used to investigate thoroughly mechanism of this coupling between the core and the 2nd core whose refractive index is higher than that of the cladding but lower than that of the core [13-15]. Accordingly, the equivalent model of refractive index profile for the *BSF* having the four refractive index regions (inner core, center dip in the inner core, outer core, and cladding) is made. By using this equivalent model of the refractive index profile of the *BSF*, the current study developed the *BSF* to scatter the light in proportion to the reciprocal of the *BR* assigned to the waveguide without eliminating the protective coating, thereby providing durability and a high recurrence. The fabricated structure of the proposed *VOFA* consists of a rectangular rubber ring including the *BSF* with a fixed *BR* in a steady state. By adjusting the mechanical pressure on the *VOFA*, the attenuation of the optical power can then be easily controlled by varying the initial *BR* of the *BSF* included in the rectangular rubber ring.

II. NUMERICAL ANALYSIS BY USING 3-DIMENSIONAL FINITE DIFFERENCE BEAM PROPAGATION METHOD

To investigate the *BSF* which has a 2nd core around the core and much larger bending loss than the *SMF* at the same bent condition, the equivalent model of the refractive index profile for the *BSF*, including the fabrication error of the process of making the fiber, such as center dip and the variation of the refractive index, was made as shown in Fig. 1. The refractive index profile of the *BSF* has four different regions which are inner core, center dip in the inner core, outer core, and cladding. Because the refractive index profile of the *BSF* is more complicated than that of the *SMF* and solving the wave equation with this refractive index profile is not simple, 3-dimensional finite-difference beam propagation method (*3-D FD-BPM*) is used to find the solution, and also to analyze the bending loss of the *BSF* with the proposed refractive index profile among the various-reported numerical techniques [13-15]. First, the governing wave equation of 3D FD-BPM is shown in equation (1),

$$\frac{\partial \phi}{\partial z} = -j\frac{1}{2kn_0}\frac{\partial^2}{\partial x^2}\phi - \alpha(x,z)\phi - jk[n^2(x,z) - n_0^2]\phi \tag{1}$$

where ϕ is the total field in a certain position, $\alpha(x, z)$ is a loss or gain term, $n(x, z)$ is a refractive index, and n_0 is a reference-refractive index in computational region. Then, a differential equation of the form can be approximated by the finite difference method, and the results are shown in equation (2),

$$\begin{aligned} A(\phi_{i,l}^{m+1} - \phi_{i,l}^{m}) = & \frac{\phi_{i-1,l}^{m} - 2\phi_{i,l}^{m} + \phi_{i+1,l}^{m} + \phi_{i-1,l}^{m+1} - 2\phi_{i,l}^{m+1} + \phi_{i+1,l}^{m+1}}{2(\Delta x)^2} \\ & + \frac{\phi_{i,l-1}^{m} - 2\phi_{i,l}^{m} + \phi_{i,l+1}^{m} + \phi_{i,l-1}^{m+1} - 2\phi_{i,l}^{m+1} + \phi_{i,l+1}^{m+1}}{2(\Delta x)^2} \\ & + B(\phi_{i,l}^{m+1} + \phi_{i,l}^{m}) \end{aligned} \tag{2}$$

where A and B are defined in (3) and (4).

$$A = \frac{j2kn_0}{\Delta z} \tag{3}$$

$$B = -jkn_0\alpha\left(i,l,m+\frac{1}{2}\right) + \frac{k^2}{2}\left[n^2\left(i,l,m+\frac{1}{2}\right) - n_0^2\right] \tag{4}$$

In addition to these, the alternating-direction implicit finite difference method (*ADIFDM*) was used to simplify the calculation procedures in 3-dimensional computational analysis. To avoid unphysical reflection into the computational domain at the interface between the computational region and the perfect matched layer (*PML*), the absorption material, which has a certain thickness, is placed in the boundary region and (σ_x, σ_x^*, 0, 0), (σ_y, σ_y^*, 0, 0) are put in the *PML* to absorb the radiation field without reflection. When the thickness of the *PML* increases, the reflection is effectively reduced, whereas the memory-need increases and the computational speed slows. Thus, the moderate-thickness of the *PML* is selected. Finally, the model of the bent fiber

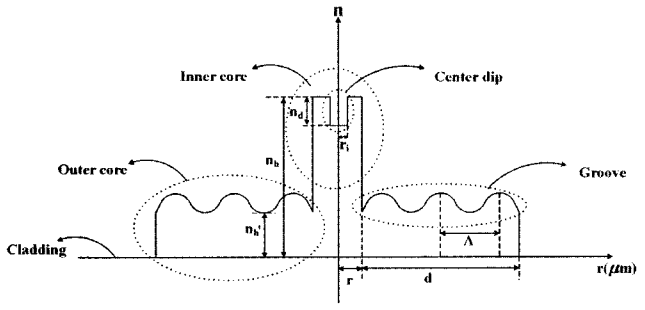

FIG. 1. The equivalent model of refractive index profile for 3D FD-BPM.

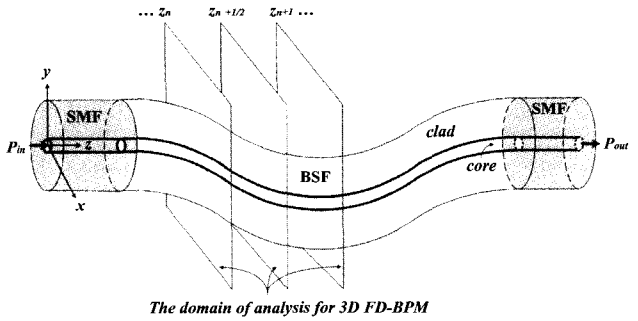

FIG. 2. The equivalent model of bent fiber for 3D FD-BPM.

was made as shown in Fig. 2, where the lattice structure is defined in the computational domain using a Δx, Δy, and Δz. The shape of the bent fiber is followed by the profile of the Gaussian function which defined in equation (6),

$$f(z) = a_0 e^{-\left(\frac{z - z_0}{w}\right)^2} \tag{6}$$

where the parameters are defined as followed: the maximal value of the Gaussian function, which is equal to bending height, a_0; the center point of the bending region, z_0, the width of the Gaussian function, which is equal to bending width, w=0.225z. Then, the investigation of the bending loss for the bent BSF with the proposed model of the refractive index profile was carried out by using *3D FD-BPM* with the following parameters: the maximal length along the x-axis, x_{max}=125 μm; the maximal length along the y-axis, y_{max}=350 μm; the maximal length along the z-axis, z_{max}=3000 μm; the size of the lattice, Δx=Δy=Δz=0.5 μm; wavelength of the light, λ=1550 nm; the radius of the fiber, r=5 μm; the radius of the center dip in the inner core, r_{in}=0.2r; the difference between the refractive index of the inner core and that of the center dip in the inner core, $n_d = \frac{1}{3} n_h$; the difference between the refractive index of the inner core and that of the cladding, n_h=0.0035; the difference between the minimal refractive index of the outer core and the refractive index of the cladding, n_h'=0.4n_h; the difference between the radius of the inner core and that of outer core, d=3r; the period of the groove showed in the outer core, Λ=3.75 μm; the difference between the maximum and the minimum in the refractive index of the outer core, n_t=0.1n_h; the refractive index of the cladding of both *SMF* and *BSF*, n_o=1.4560; and the refractive index of the core in the *SMF*, n_{SMF}=1.4615. The bending loss of the *BSF* according to the variation of a_0 is investigated by using *3D FD-BPM* and compared with the bending loss of the *SMF* and the fiber which consists of core, whose refractive index is 0.67 times of the

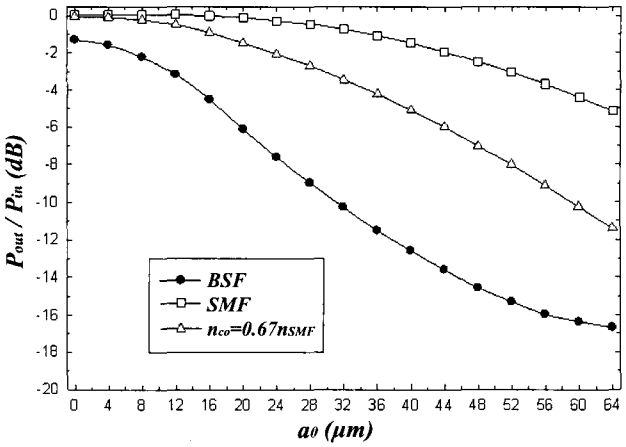

FIG. 3. The bending loss according to a_0.

refractive index of the core in *SMF*, and cladding. The numerical analysis by using *3D FD-BPM* is shown in Fig. 3. According to the figure, the bending loss of the *BSF* is 5 times more than the bending loss of the *SMF*, -3 dB, and the fiber which consists of the core, whose refractive index is 0.67 times of the refractive index of the core in the *SMF*, and cladding shows 2.7 times more of the bending loss of *SMF* at the same bending, a_0=52 μm. The 3-dimensional mode field profile of the *BSF*, which is coupled with the *SMF* at both ends, is investigated by using *3D FD-BPM*, so the result of the investigation with *3D FD-BPM* is shown in Fig. 4. The 3-dimensional mode field profile of the *BSF* is obtained at the center point of the bending region and the output. According to the mode field profile, the optical power of the inner core is easily coupled with the outer core with the very low bending height, a_0=8 μm, then it escapes from the outer core to cladding. However, the optical power of the *BSF* is conserved when the bending is not given to the *BSF*. The cross sectional view of the mode field profile of the *BSF* at the output is also investigated and compared with that of the really fabricated *BSF* in Fig. 5. According to the profile by utilizing *3D FD-BPM*, the center-dip, the boundary between the inner core and the outer core, and the variation of the refractive index of the outer core are outstanding by the shape of the dark circle. In the case of the bent fiber, the optical power in the inner core and the outer core almost disappears. These phenomena are also shown in the profile of the really fabricated *BSF* with proposed refractive index profile. On the basis of all the results of the numerical analysis by using *3D FD-BPM*, adding the 2nd core denoted as outer core around the core described as inner core is another effective method of fabricating the *BSF*. As a result, the *BSF* with the proposed refractive index model can make higher bending loss than that of the *SMF*, without removing the protective coating.

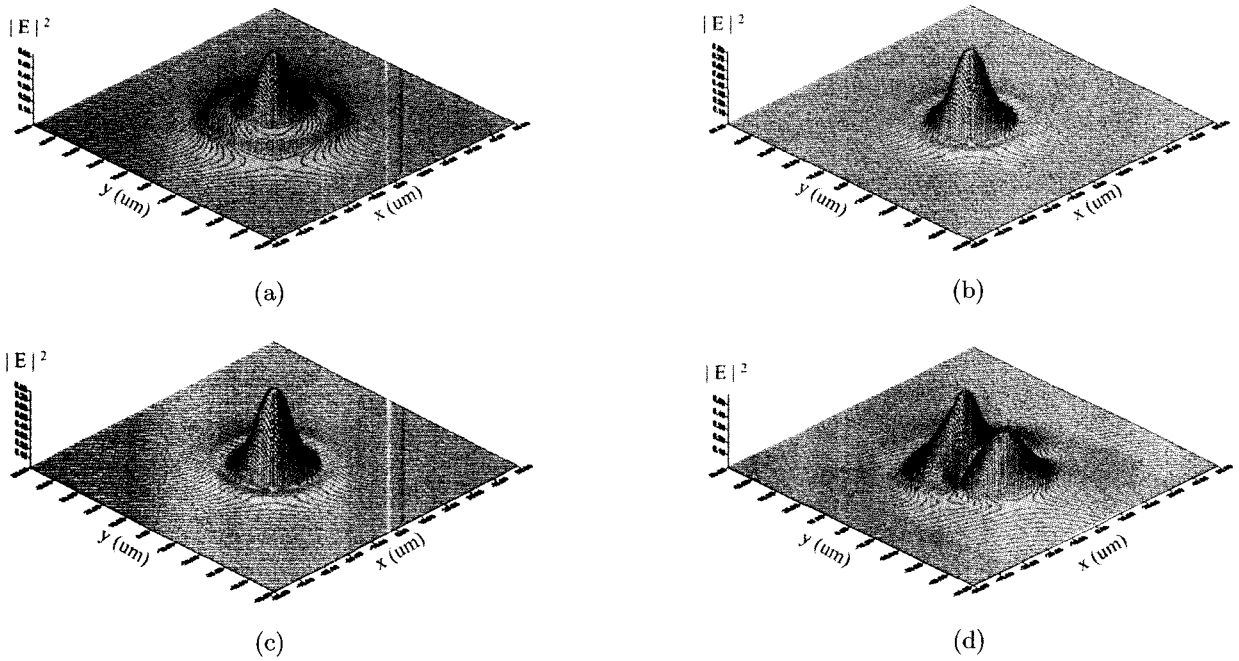

FIG. 4. The three dimensional mode field profile of the BSF. (a) Center of the bending, a_0=0 ㎛, (b) Output, a_0=0 ㎛, (c) Center of the bending, a_0=8 ㎛, (d) Output, a_0=8㎛

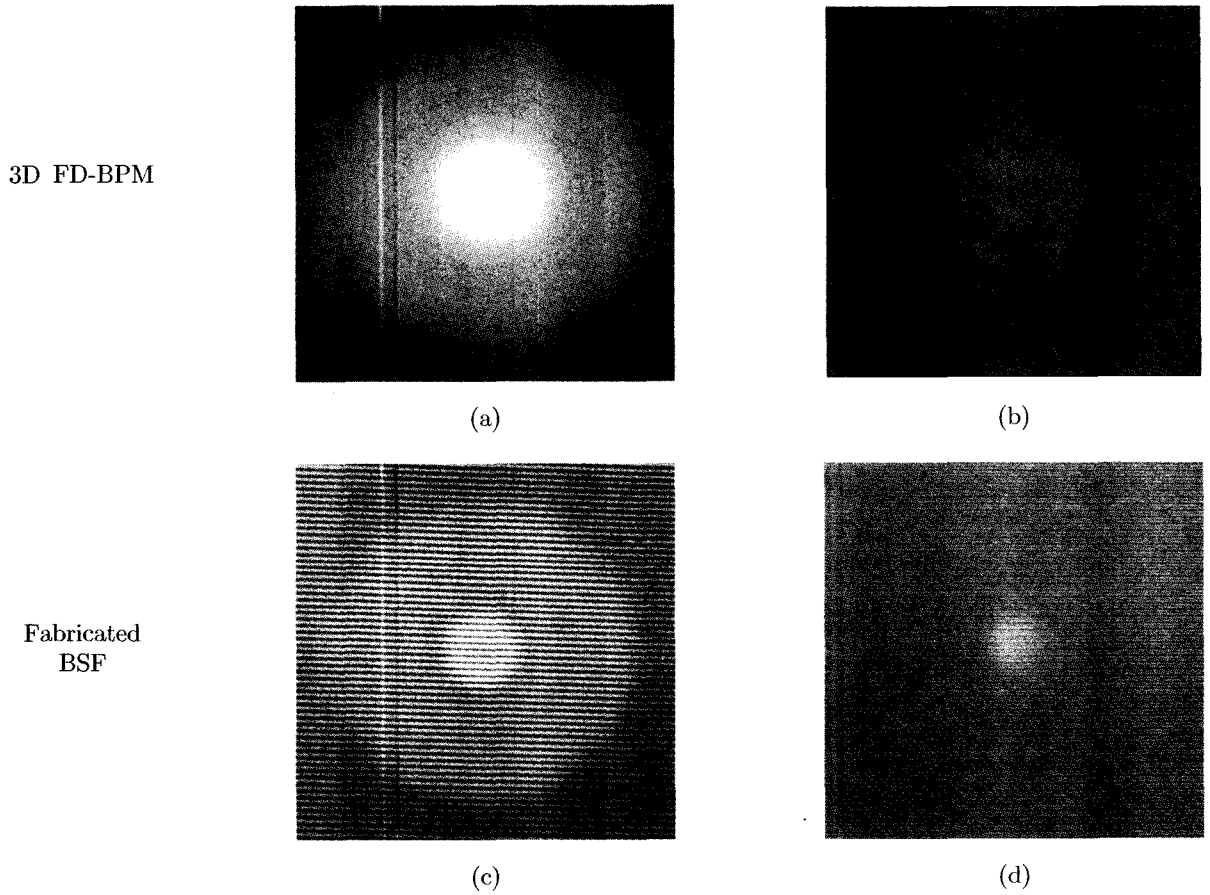

FIG. 5. The cross sectional view of the mode field profile of the BSF at the output. (a) a_0=0㎛, (b) a_0>>64㎛, (c) nc bending, (d) sharp bending

III. DEVICE FABRICATION AND EXPERIMENT

By using the equivalent model which is made on the basis of the numerical analysis with *3-D FD-BPM*, the *BSF* was fabricated, and the refractive index profile of the fabricated *BSF*, which is shown in Fig. 6, was measured by using a fiber analyzer (*NR* 9200). According to Fig. 6, the measured refractive index profile of the *BSF* is similar to the proposed refractive index profile of the *BSF*, which considers the fabrication error in the process of the making the fiber. The refractive index profile of the fabricated *BSF* is divided into four regions which are inner core, center dip in the inner core, outer core, and cladding. The radius of the outer core is about four times of the radius of the inner core, and the center-dip depth is about one third of the refractive index of the inner core. The insertion loss of the *BSF* was about 0.68 *dB*, while the return loss of the *BSF* was less than -60 *dB*. The proposed *VOFA* consists of the *BSF* and rectangular ring made of rubber with a general elastic coefficient, and the *BSF* in the rectangular rubber ring is initially fixed with a certain *BR* to give a constant attenuation in a steady state. In addition, to obtain a reliable recurrence for the *BR*, the central point of the *BR* is fixed to the ridge of the upper part of the rectangular rubber ring. The dimensions of the rectangular rubber ring were as follows: W=25 *mm*, L=10 *mm*, H=30 *mm*, w=2 *mm*, and h=2 *mm*. A rectangular rubber ring with a high elastic coefficient can provide a reliable recurrence for the proposed *VOFA*, as the ring easily returns to its original form when the mechanical perturbation on the surface of the rectangular rubber ring disappears. In the experiments with the proposed *VOFA*, the *BR* of the *BSF* was set at 10 *mm* in a steady state for good recurrence. Plus, the wavelength range of the optical spectrum analyzer (*OSA*) was set at 1540 *nm* to 1560 *nm* to measure the optical power of the *EDFA* with a 1480 *nm* pump diode when the wavelength resolution was 0.2 *nm*. The experimental results for the effect of bending and polarization on the *BSF* were compared with those for a single mode fiber (*SMF*), as shown in Fig. 7. The optical power attenuation of the *BSF* was found to be more proportional to the reciprocal of the *BR* than that of the *SMF*. The maximum attenuation was about 32 *dB* when the *BR* was 10 *mm* at a wavelength of 1550 *nm*, meanwhile the polarization loss was nearly the same as that with the *SMF*. As such, a *BSF* would appear to be suitable for a *VOFA* to attenuate the optical power based on being controlled by the *BR* of the *BSF*. The fabricated *VOFA* using a *BSF* is shown in Fig. 8. By applying mechanical pressure to the rectangular rubber ring, the *BR* of the *BSF* in the ring can be easily changed, as shown in Fig. 9. When the mechanical pressure on the rectangular rubber ring is increased, the *BR* of the *BSF* in the ring also increases incrementally, thereby increasing the confinement of light at the output of the *VOFA*. As a result, the proposed *VOFA* can attenuate an optical power until -38 *dB* based on adjusting the mechanical

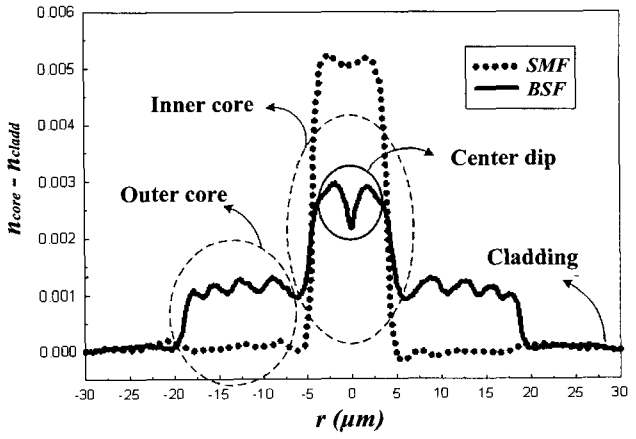

FIG. 6. The measured refractive index profile of the BSF and the SMF.

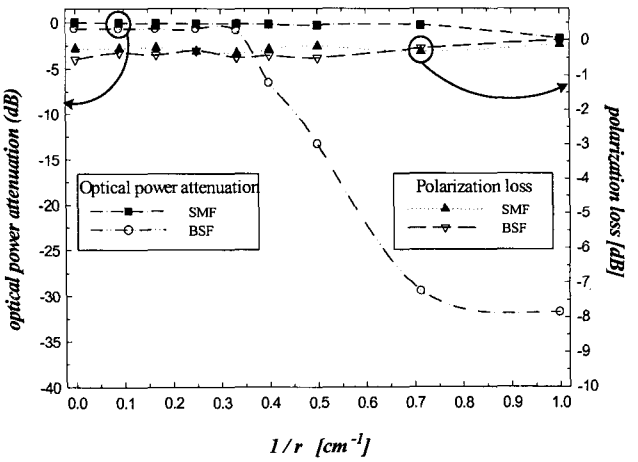

FIG. 7. Typical attenuation of light and polarization loss versus BR at 1550 nm.

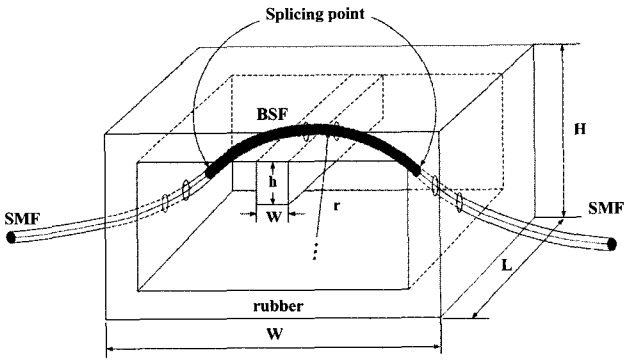

FIG. 8. Structure of VOFA using rectangular rubber ring.

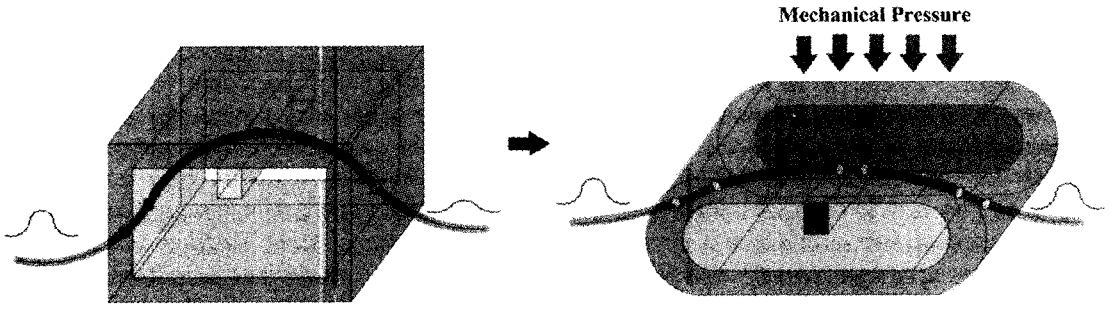

FIG. 9. Variation of BR in VOFA according to mechanical pressure on rectangular rubber ring.

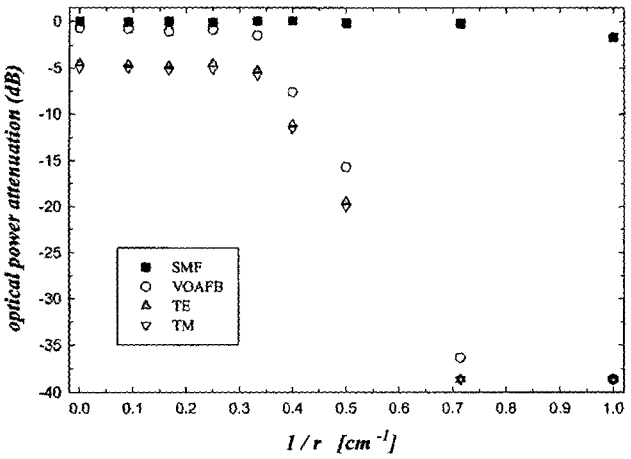

FIG. 10. Typical optical power attenuation of VOFA versus bend radius at 1550 nm.

pressure on the rectangular rubber ring with the *BSF*. Fig. 10 shows that the optical power can be easily controlled by the variance of the *BR*, which is dependent on the mechanical pressure. Overall, the optical power within the tested wavelength range was uniformly attenuated until -10 *dB* in proportion to the mechanical pressure on the *VOFA*. Yet, below -10 *dB* in the tested wavelength range, the optical power level fluctuated. This phenomenon is regarded as the wavelength selectivity of the *BSF*. Based on the experimental results for the dependence of the polarization, the polarization loss of the proposed *VOFA* was about -0.5 *dB*. In addition to the encouraging experimental results, the VOFA also has other advantages, including no propagation loss, reliable recurrence, and lost cost mass production.

IV. CONCLUSION

The *BSF*, which is used in a variable optical fiber attenuator (*VOFA*) along with the simple fabrication process using a rectangular rubber ring with an elastic coefficient, is proposed by adding 2^{nd} core defined as outer core around the 1^{st} core equivalent to the inner core. Therefore, if the fabrication error of the process in making the fiber is considered, the refractive index profile of the *BSF* has the four different regions, which are inner core, center dip in the inner core, outer core, and the cladding region, when considering the fabrication error of the process in making the fiber. The 3 dimensional mode field profile of the *BSF* is obtained by utilizing *3D FD-BPM* and the cross sectional view of the mode field profile at the output of the *BSF* is also investigated. According to the mode field profile, the mode of the inner core is easily coupled with the outer core at the very weak bending, and then escapes from the outer core to cladding, so the *BSF* with the proposed refractive index profile shows 5 times of the bending loss of the *SMF* at the same bending condition. By using the *BSF* with the proposed refractive index profile which is made on the basis of the numerical results with *3D FD-BPM*, the *BSF* is really fabricated and the refractive index profile of the fabricated *BSF* is measured, which is similar to the proposed refractive index profile of the *BSF*, where the fabrication error is included. When the *BR* of the *BSF* with a protective coating is varied from 10 *mm* to 40 *mm*, the scattering of light in the core also changes easily. The attenuation of the optical power is also proportional to the reciprocal of the *BR* of the *BSF*, and in the current study, the optical power relative to the *BR* was about 10 dB/cm in the conventional band region. The proposed *BSF* also exhibits a superior recurrence and is not significantly affected by temperature changes as its protective coating does not have to be removed. Using these features of the *BSF*, the proposed *VOFA* produced reliable attenuation with a dynamic range of more than 38 *dB* in the conventional band region, return loss of less than -60 *dB*, and *PDL* of about 0.5 *dB*. As such, the proposed *VOFA* is appropriate for application to common optical networks. In addition, the proposed *VOFA* has a very simple structure, low production cost, and provides easy mechanical control of the optical power. When the rectangular rubber ring is made with a different elastic coefficient, the features of the proposed *VOFA* can be easily and effectively controlled. In addition to the experimental results with a variable

optical fiber attenuator, the proposed *VOFA* can be also used as an optical pressure sensor with a high sensitivity to mechanical pressure on the rectangular rubber ring with a bent *BSF*. Furthermore, the proposed BSF has many potential uses in other optical sensing applications.

*Corresponding author : dhlee922@palgong.knu.ac.kr

REFERENCES

[1] Yasuji Murakami and Haruhiko Tsuchiya, "Bending losses of coated single-mode optical fibers," *J. of Quantum Electronics*, vol. QE-14, no. 7, pp. 495-501, 1978.

[2] Katsumi Morishita, Yasuyuki Kondoh, and Nobuaki Kumagai, "On the accuracy of scalar approximation technique in optical fiber analysis," *IEEE Transactions on Microwave Theory and Techniques*, vol. MTT-28, no. 1, pp. 33-36, 1980.

[3] Alun J. Harris and Peter F. Castle, "Bend loss measurements on high numerical aperture single-mode fibers as a function of wavelength and bend radius," *J. of Lightwave Technology*, vol. LT-4, no. 1, pp. 34-40, 1986.

[4] J. R. Simpson, R. H. Stolen, F. M. Sears, W. Pleibel, J. B. Macchesney, and R. E. Howard, "A single-polarization fiber," *J. of Lightwave Technology*, vol. LT-1, no. 2, pp. 370-373, 1983.

[5] Sean M. Garner and Steve Caracci, "Variable optical attenuator for large-scale integration," *IEEE Photonics Technology Letters*, vol. 14, no. 11, pp. 1560-1562, 2002.

[6] Joseph E. Ford, James A. Walker, Dennis S. Greywall, and Keith W. Goossen, "Micromechanical fiber-optic attenuator with 3 μs response," *IEEE J. of Lightwave Technology*, vol. 9, no. 9, pp. 1663-1670, 1998.

[7] F. Chollet, M. de Labachelerie, and H. Fujita, "Electromechanically actuated evanescent optical switch and polarization independent attenuator," *IEEE MEMS 98. Proceedings*, pp. 476-481, 1998.

[8] Tetsuya Mizumoto and Yoshiyuki Naito, "Waveguide-type optical attenuator," *IEEE J. of Lightwave Technology*, vol. LT-3, no. 4, pp. 841-843, 1985.

[9] Sang-Shin Lee, Yong-Sung Jin, and Yung-Sung Son, "Variable optical attenuator based on a cutoff modulator with tapered waveguides in polymers," *IEEE J. of Lightwave Technology*, vol. 17, no. 12, pp. 2556-2561, 1999.

[10] Val Morozov, Haining Fan, Louay Eldada, Long Yang, and Yuan Shi, "Fused fiber optic variable attenuator," *Optical Fiber Communication Conference*, vol. 4, pp. 22-24, 2000.

[11] Mitsuo Takahashi, "Variable light attenuator of improved air-gap type with extremely low returning light," *IEEE Conference Proceedings*, pp. 947-950, 1994.

[12] T. Hashimoto and M.S. Yataki, "Variable optical fiber attenuators," *IEEE CLEO Pacific Rim*, pp. 1151-1152, 1999.

[13] R. Clauberg and P. Von Allmen, "Vectorial beam-propagation method for integrated optics," *Electron. Lett.*, vol. 27, no. 8, pp. 654-655, Apr. 11, 1991.

[14] Fabrizio Fogil, Gaetano Bellanca, Paolo Bassi, Iain Madden, and Walter Johnstone, "Highly Efficient Full-Vectorial 3-D BPM modeling of fiber to planar waveguide couplers," *J. Lightwave Technol.*, vol. 17, no. 1, pp. 136-143, 1999.

[15] W. P. Huang, C. L. Xu, W. Lui, and K. Yokoyana, "The prefectly matched layer (PML) boundary condition for the beam propagation method," *IEEE Photon, Technol. Lett.*, vol. 8, pp. 649-651, 1996.